EFFECT OF ANISOTROPY ON THE VIBRATION CHARACTERISTICS OF COMPOSITE SHELLS OF REVOLUTION

Altan Kayran, Erdem Yavuzbalkan
Department of Aerospace Engineering, METU, Ankara, Turkey

Keywords: *anisotropy, laminated composites, shell of revolution, vibrations*

Abstract

The effect of anisotropy on the natural frequencies and modes shapes of laminated composite shells of revolution is studied by a semi-analytical solution method which exploits the combination of the numerical integration technique, and a modified frequency trial method. The governing shell of revolution equations comprise the full anisotropic form of the constitutive relations, including first order transverse shear deformation, and all components of translatory and rotary inertia. To study the coupled effect of anisotropy, geometry and boundary conditions on the vibration characteristics of anisotropic shells of revolution, numerical results are obtained for different shell geometries with different boundary conditions. Emphasis is placed on the effect of fibre orientation angle, stacking sequence, and coupling stiffness coefficients on the natural frequencies and modes shapes of anisotropic shells of revolution.

1 Introduction

Laminated composite shell structures are finding ever increasing application areas in many engineering disciplines due to their superior strength to weight, stiffness to weight ratio and corrosion resistant properties, among others, compared to structures made of metallic isotropic materials. Several solution strategies have been used for the vibration analysis of laminated composite shells of revolution. The most commonly used approach is based on the representation of the shell variables by a Fourier series in the circumferential coordinate, combined with the use of a numerical discretization technique such as finite elements, or numerical integration in the meridional direction. The main emphasis of most of the past studies has concentrated more on the solution methodology used in the vibration analysis of anisotropic shells of revolution, rather than a comprehensive study of the effect of anisotropic nature of the shell wall on the free vibration characteristics [1-5].

The main objective of the present paper is to study the effect of anisotropy on the natural frequencies and mode shapes of shells of revolution. The semi-analytical method of solution which is used in this study is utilizes the multisegment numerical integration technique for the solution of free vibration problem of anisotropic shells of revolution through the use of finite exponential Fourier transform of the fundamental shell equations. Solution procedure is based on a modified frequency trial method [6], which processes on the numerically integrated transformed fundamental system of equations of anisotropic shells of revolution. The governing equations of include first order transverse shear deformation, and all components of translatory and rotary inertia.

To understand the coupled effect of anisotropy, geometry and boundary conditions on the vibration characteristics of anisotropic shells of revolution, numerical results are obtained for different shell geometries with different boundary conditions, and for different vibration modes. The results focus on the effect of fiber orientation angle, stacking sequence, and coupling stiffness coefficients on the natural frequencies and mode shapes of macroscopically anisotropic shells of revolution. Relations are established with regard to the combined effect of stiffness coefficients of the anisotropic shells of revolution and dominant strain energy contributions at particular vibration modes, on the natural frequencies.

2 Governing Equations

In the present study, the shell of revolution equations, governing the vibration of anisotropic shells of revolutions, consist of strain displacement relations of the Reissner-Naghdi shell theory [7], dynamic equilibrium equations[6,8] and full

macroscopically anisotropic form of the constitutive relations [9]. For laminated composite structures, full anisotropic form of the constitutive equations relating the stress resultants to mid surface strains ($\varepsilon^0_{\phi\phi}, \varepsilon^0_{\theta\theta}, \gamma^0_{\phi\theta}$) and curvatures ($\kappa_{\phi\phi}, \kappa_{\theta\theta}, \kappa_{\phi\theta}$) are given in matrix form by Eq. 1.

$$\begin{Bmatrix} N_{\phi\phi} \\ N_{\theta\theta} \\ N_{\phi\theta} \\ M_{\phi\phi} \\ M_{\theta\theta} \\ M_{\phi\theta} \end{Bmatrix} = \begin{bmatrix} A_{11} & A_{12} & A_{16} & B_{11} & B_{12} & B_{16} \\ A_{12} & A_{22} & A_{26} & B_{12} & B_{22} & B_{26} \\ A_{16} & A_{26} & A_{66} & B_{16} & B_{26} & B_{66} \\ B_{11} & B_{12} & B_{16} & D_{11} & D_{12} & D_{16} \\ B_{12} & B_{22} & B_{26} & D_{12} & D_{22} & D_{26} \\ B_{16} & B_{26} & B_{66} & D_{16} & D_{26} & D_{66} \end{bmatrix} \begin{Bmatrix} \varepsilon^0_{\phi\phi} \\ \varepsilon^0_{\theta\theta} \\ \gamma^0_{\phi\theta} \\ \kappa_{\phi\phi} \\ \kappa_{\theta\theta} \\ \kappa_{\phi\theta} \end{Bmatrix} \qquad (1)$$

In addition, transverse shear stress resultants are related to transverse shear strains ($\gamma^0_\theta, \gamma^0_\phi$) by Eq. 2.

$$\begin{Bmatrix} Q_\theta \\ Q_\phi \end{Bmatrix} = \begin{bmatrix} As_{44} & As_{45} \\ As_{45} & As_{55} \end{bmatrix} \begin{Bmatrix} \gamma^0_\theta \\ \gamma^0_\phi \end{Bmatrix} \qquad (2)$$

For a doubly curved shell of revolution, ϕ and θ represent the curvilinear coordinates along the meridian and tangential directions of the shell of revolution, respectively. In Eqs. 1 and 2, the coefficients given in the square matrix expressions represent the stiffness coefficients of the shell wall, which is built up from individual layers of arbitrary fiber orientation, and they are defined in the usual manner [9].

In the derivation process of dynamic equilibrium equations, application of Hamilton's principle also generates conditions on the boundary displacements, and boundary stress resultants which are applied at the constant meridional coordinate (ϕ =constant) of a shell of revolution. For the free vibration problem, boundary conditions are given by setting one of the variables given inside the parenthesis of the shell variable pairs in Eqs. 3 and 4 to zero [10].

$$(N_{\phi\phi}, u^0_\phi), (N_{\phi\theta}, u^0_\theta), (Q_\phi, w^0) = 0 \qquad (3)$$

$$(M_{\phi\phi}, \beta_\phi), (M_{\phi\theta}, \beta_\theta) = 0 \qquad (4)$$

In Eqs. 3 and 4, $u^0_\phi, u^0_\theta, w^0$ represent the mid surface displacements at the reference surface of the shell along the meridian, circumferential, and transverse directions, respectively. β_ϕ and β_θ represent the rotations of a transverse normal about θ and ϕ curvilinear coordinates, respectively.

In order to apply the numerical integration technique to the solution of the vibration problem, strain displacement relations, dynamic equilibrium equations, and anisotropic constitutive relations are brought into a fundamental system of equations which can be expressed as in Eq. 5.

$$\frac{\partial\{\psi(\phi,\theta,t)\}}{\partial\phi} = \{f(\phi,\theta,t)\} \qquad (5)$$

In Eq. 5 $\{\psi\}$ is a vector representing the fundamental shell variables, which enter into the appropriate boundary conditions at a rotationally symmetric edge of the rotationally symmetric shell. Therefore, vector $\{\psi\}$ consists of the variables given by Eqs. 3 and 4. It is customary to organize the fundamental shell variable vector such that the first five elements of the vector are the displacements and rotations, and the last five elements are the stress resultants. The right hand side of Eq.5 is a function of the fundamental shell variables, first and second θ derivatives of some of the fundamental shell variables, stiffness coefficients of the anisotropic shell wall, and two radii of curvature of the doubly curved shell of revolution. The system of equations given by Eq.5 is derived by the complex manipulation of the strain displacement relations, dynamic equilibrium equations, and full anisotropic form of the constitutive relations. For anisotropic shells of revolution, the derivation of the fundamental system of equations in the form of Eq.5 is explained in detail in Ref. 6.

For anisotropic shells of revolution, which are characterized by the constitutive relations given by Eqs. 1 and 2, the existence of full coupling stiffness coefficients precludes the uncoupling of fundamental system of shell equations, describing the symmetric and antisymmetric responses with respect to circumferential coordinate, by the classical sine or cosine Fourier decomposition of the fundamental shell variables. Therefore, to accomplish the uncoupling of the circumferential coordinate from the fundamental system of equations, each fundamental variable is expanded in complex Fourier series as shown in Eq. 6.

$$\{\psi_n(\phi)\} = \int_0^{2\pi} \{\psi(\phi,\theta)\} \frac{e^{-in\theta}}{2\pi} = \{\psi_{nc}(\phi)\} - i\{\psi_{ns}(\phi)\} \qquad (6)$$

In Eq.6, it is assumed that for the free vibration analysis, the time dependence of each quantity in

synchronous motion appears in a factor $e^{i\omega t}$, where ω is the natural frequency. Back transformation of the fundamental variable vector is achieved by Eq.7.

$$\{\psi(\phi,\theta)\}=\sum_{n\to-\infty}^{n\to+\infty}\{\psi_n(\phi)\}e^{in\theta} \qquad (7)$$

It is clear form Eq. 6 that the application of finite exponential Fourier transform, results in doubling of the number of fundamental variables. Thus, finite exponential Fourier transform of Eq. 5 yields a system of twenty ordinary differential equations in terms of the transformed fundamental shell variables, and this system of equations is given in Eq. 8.

$$\frac{d}{d\phi}\{\psi\}=\frac{d}{d\phi}\begin{Bmatrix}\psi^{(1)}(\phi)\\ \psi^{(2)}(\phi)\end{Bmatrix}=[K(n,\omega,\phi)]\begin{Bmatrix}\psi^{(1)}(\phi)\\ \psi^{(2)}(\phi)\end{Bmatrix} \qquad (8)$$

In Eq. 8, n is the circumferential wave number, and the fundamental variable vector is partitioned such that the first half consists of cosine and sine parts of the displacements and rotation of the reference surface of the shell of revolution, and the second half consists of the cosine and sine parts of the stress resultants. The elements of the coefficient matrix K for anisotropic shells of revolution are given in Ref.6. Similarly, application of the finite exponential Fourier transform to Eqs. 3 and 4, results in doubling the number of boundary conditions, which are defined in terms of cosine and sine parts of the fundamental shell variables. Eq. 8, together with the boundary conditions expressed in terms of transformed fundamental variables, specified at the two boundary edges of an anisotropic shell of revolution, form an eigenvalue problem for the eigenvectors which are the transformed displacements, rotations, and stress resultants.

3 Method of Solution

The solution for the natural frequencies and variation of shell variables along the meridian of the shell of revolution is accomplished by employing the multisegment numerical integration technique [11]. In the multisegment numerical integration technique, the shell is divided into M number of segments in the meridional direction, and the solution to Eq. 8 can be written as in Eq. 9.

$$\{\psi(\phi)\}=[T(n,\omega,\phi)]_i\{\psi(\phi_i)\} \quad (i=1,2,...M) \qquad (9)$$

In Eq. 9, transfer matrices T_i are obtained from the initial value problems defined in each segment i by Eq. 10 subject to initial condition given by Eq. 11.

$$\frac{d}{d\phi}[T(n,\omega,\phi)]_i=[K(n,\omega,\phi)][T(n,\omega,\phi)]_i \qquad (10)$$

$$[T(n,\omega,\phi_i)]_i=[I] \qquad (11)$$

In the present study, the initial value problems defined by Eqs. 10 and 11 are solved by the numerical integration of the equations by the IMSL subroutine DIVPAG. Continuity requirements of the fundamental variables at the end points of the shell segments ($i=1,2,...M$), lead from Eq. 9 to the partitioned matrix equation given by Eq. 12.

$$\begin{Bmatrix}\psi^{(1)}\\ \psi^{(2)}\end{Bmatrix}_{i+1}=\begin{bmatrix}T_i^{(1)} & T_i^{(2)}\\ T_i^{(3)} & T_i^{(4)}\end{bmatrix}_{i+1}\begin{Bmatrix}\psi^{(1)}\\ \psi^{(2)}\end{Bmatrix}_i \qquad (12)$$

For computational ease, the rows of the fundamental variable vector ψ at both ends of the shell, ϕ_1 and ϕ_{M+1}, are adjusted such that for the anisotropic shell of revolution, the first 10 elements of $\{\psi(\phi_1)\}$ and the last 10 elements of $\{\psi(\phi_{M+1})\}$ are the prescribed boundary conditions. In the following, to keep the uniformity of the notation used for the partitioned fundamental variable vector, the boundary conditions are also represented by the same vector notation defined by Eq. 8. Therefore, at both ends of the shell of revolution, the boundary conditions are expressed by Eq. 13.

$$\left\{\psi^{(1)}(\phi_1)\right\}=\left\{\psi^{(2)}(\phi_{M+1})\right\}=0 \qquad (13)$$

The solution for the eigenvalue problem requires the writing out of matrix equations, Eq. 12, in each interval i separately, and bringing the whole equation set into an upper diagonal matrix equation by Gauss elimination.

$$\begin{bmatrix}E_1 & -I & 0 & . & . & 0\\ 0 & C_1 & -I & 0 & . & 0\\ . & 0 & . & . & . & .\\ . & . & 0 & . & . & .\\ 0 & . & . & 0 & E_M & -I\\ 0 & . & . & 0 & 0 & C_M\end{bmatrix}\begin{Bmatrix}\psi^{(2)}(\phi_1)\\ \psi^{(1)}(\phi_2)\\ .\\ .\\ \psi^{(2)}(\phi_M)\\ \psi^{(1)}(\phi_{M+1})\end{Bmatrix}=0 \qquad (14)$$

In Eq. 14, the (10X10) matrices E_1 and C_1 are evaluated successively from Eqs. 15 and 16.

$$E_1=T_1^{(2)} \qquad (15)$$

$$C_1 = T_1^{(4)} E_1^{-1} \tag{16}$$

For the remaining shell segments $(i = 2,3,...,M)$, the (10X10) matrices E_i and C_i are evaluated successively from Eqs. 17 and 18.

$$E_i = T_i^{(2)} + T_i^{(1)} C_{i-1}^{-1} \tag{17}$$

$$C_i = \left(T_i^{(4)} + T_i^{(3)} C_{i-1}^{-1} \right) E_i^{-1} \tag{18}$$

Natural frequencies are then determined by requiring the non-trivial solution of the last row of Eq. 14, and setting the determinant of the coefficient matrix to zero.

$$\left| C_M \right|_{10x10} = 0 \tag{19}$$

Assuming that a particular natural frequency is determined from Eq. 19, then from the last row of Eq. 14, $\psi^{(1)}(\phi_{M+1})$ is determined up to an arbitrary constant. The remaining unknown fundamental variables at each ends of the shell segments can then be calculated successively from the rows of Eq. 14.

Natural frequencies are calculated by tracing the determinant of the characteristic matrix C_M for incremented values of the frequency estimates within a frequency range of interest. When the finite exponential Fourier transform of the fundamental shell equations was used, it was observed that determinant of the characteristic matrix does not change sign, but rather it is always positive, and vanishes at the natural frequency [6]. For a typical shell of revolution, the determinant of the characteristic matrix versus the non-dimensional frequency is plotted in Fig. 1, in a range where a natural frequency actually resides.

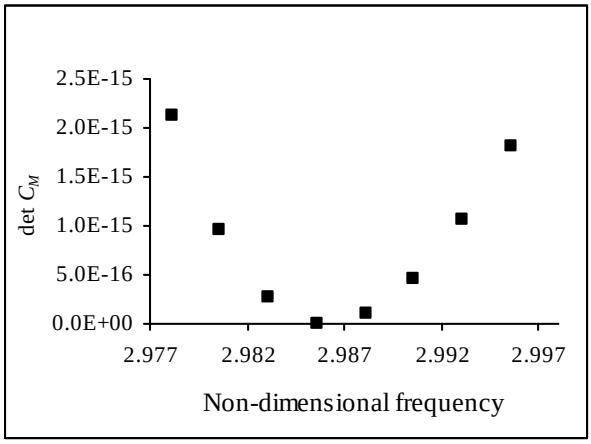

Fig. 1. Variation of the characteristic determinant

To extract the natural frequency, a slope change detection algorithm in combination with inverse interpolations was devised. The method essentially relies on checking the slope change of the determinant of the characteristic matrix, and detecting an interval where a natural frequency resides. Once an interval is determined, by successive inverse interpolations natural frequency is extracted.

4 Study of the Effect of Anisotropy on the Vibration Characteristics

4.1 Effect of Fibre Orientation Angle

By implementing the semi-analytical method of solution described, a sample study is performed for the effect of fibre orientation angle on the natural frequencies of a truncated spherical shell which is clamped at the inner rim and free at the outer edge. The truncated sphere is assumed to have a radius of 1 m, and overall thickness of 5.76 mm, and the shell is assumed to be clamped at the meridian angle of $\phi = 10^o$, and free at the outer edge, $\phi = 70^o$. Material is taken as high modulus graphite/epoxy with E_1 =207.35GPa, E_2 =5.18GPa, ν_{12} =0.25, $G_{12} = G_{13} = G_{23} = 3.11$ GPa, ρ =1524.47 kg m^{-3}. Shell wall is constructed from 48 layers each having the same fibre orientation angle α, and ply thickness of 0.12 mm. Fig. 2 shows the variation of the lowest scaled non-dimensional natural frequency (W*100) with respect to fibre orientation angle, corresponding to different circumferential modes.

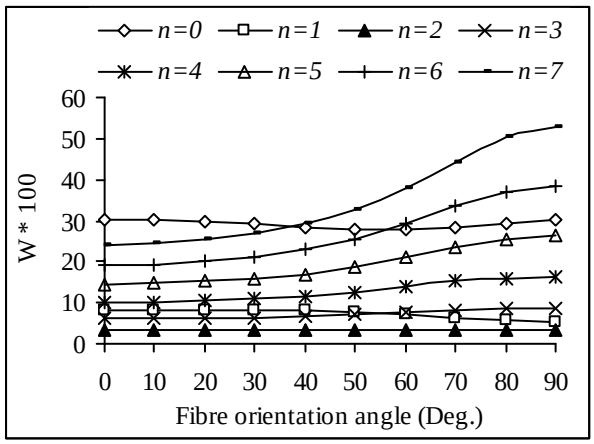

Fig. 2. Variation of natural frequency with respect to fibre orientation; clamped-free case

In Fig. 1 non dimensional frequency W is calculated according to Eq. 20.

$$W = \left(\omega h \sqrt{\rho / E_1}\right) * 10^3 \qquad (20)$$

In Eq. 20, h represents the thickness of the shell wall.

Fig.3 gives the variation of the natural frequency of the same truncated spherical shell which is clamped at both inner and outer rims.

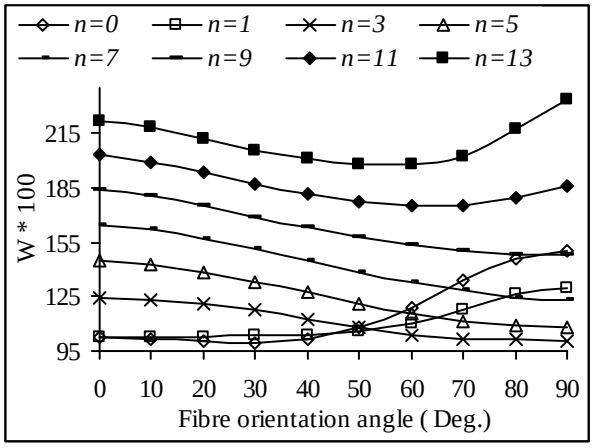

Fig. 3. Variation of natural frequency with respect to fibre orientation; clamped-clamped case

Figs. 2 and 3 reveal that, eventually at higher circumferential modes, shells with layers having circumferentially dominant fibre orientation start to have higher natural frequencies. This behaviour is attributed to the dominance of bending strain energy contribution to the total strain energy at high circumferential wave numbers [12]. At high circumferential wave numbers, circumferential slices taken from the shell of revolution resemble to a beam with $2n$ nodal points along the circumference. Therefore, circumferential bending stiffness coefficients (D_{22}), become the dominant factor affecting the natural frequencies. However, it is noticed that shell geometry and boundary conditions also have significant effect on variation of the natural frequencies with the fibre orientation angle. It is seen that, compared to the clamped-free spherical shell, natural frequencies of clamped-clamped spherical shell increase with fibre orientation angle at considerably higher circumferential wave numbers. For the clamped-clamped shell, the effect of higher meridional bending stiffness (D_{11}) achieved with meridional fibre orientation, on the natural frequencies is apparently far more significant compared to the effect of higher circumferential bending stiffness (D_{22}) achieved with circumferential fibre orientation, on the natural frequencies. For instance, for the clamped-free case, natural frequencies start to increase with the fibre orientation angle after n =2. However, for the spherical shell with both edges clamped, for circumferential wave numbers less than 11, natural frequencies decrease with increasing fibre orientation angle. At low circumferential wave numbers, compared to bending strain energy the extensional strain energy is more dominant in its contribution to the total strain energy [12]. Therefore, at low circumferential wave numbers, relative differences among the extensional stiffness coefficients of the laminates with different fibre orientations also start to be effective in the variation of the natural frequency with the orientation angle.

Figs. 4 and 5 show effect of fibre orientation on the fundamental lateral displacement mode shapes for the spherical shell, which is clamped at both edges, for the circumferential mode n =1.

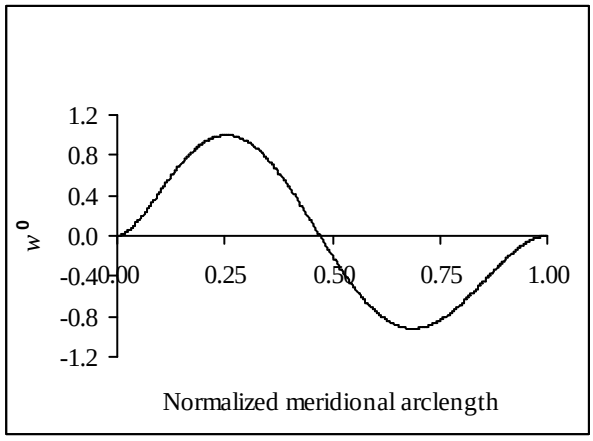

Fig. 4. Fundamental lateral displacement mode shape $\left(w^0\right)$; n =1, $\alpha = 0^o$

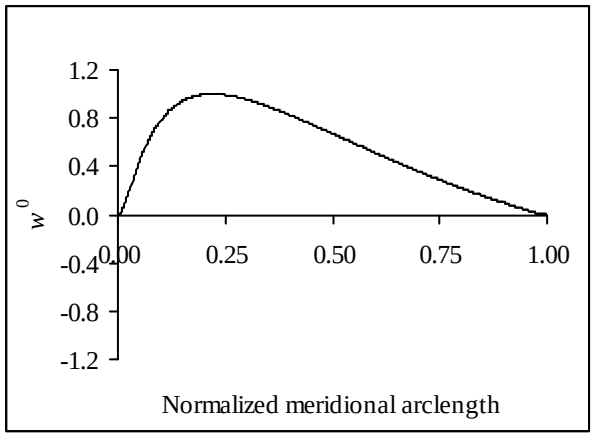

Fig. 5. Fundamental lateral displacement mode shape $\left(w^0\right)$; n =1, $\alpha = 90^o$

It is noticed that for the 0^o fibre orientation case, there is a single nodal point along the meridian of the shell, but for the 90^o fibre orientation case, node disappears. It should be noted that for the 0^o and 90^o fibre orientation cases, the sine part of the lateral displacement vanishes and the cosine part represents the actual physical lateral displacement.

4.2 Effect of Stacking Sequence

The effect of stacking sequence on the natural frequencies of laminated composite shells is demonstrated for a cylindrical shell (radius: 0.21m, length: 1.2 m), which is clamped at both edges. Same high modulus graphite/epoxy material, as in spherical shell case, is assumed to be used for the ply material, with the same ply thickness of 0.12 mm. Six different symmetric lay-ups, listed in Table 1, are used to build the cylindrical shell wall. Lay-ups are built from different combinations of 0^o, $\pm 45^o$, and 90^o plies.

Table 1. List of lay-ups

Lay-up	Stacking sequence
1	$[0_2^0/90_2^0/\pm 45_2^0]_s$
2	$[0_2^0/\pm 45_2^0/90_2^0]_s$
3	$[\pm 45_2^0/0_2^0/90_2^0]_s$
4	$[\pm 45_2^0/90_2^0/0_2^0]_s$
5	$[90_2^0/\pm 45_2^0/0_2^0]_s$
6	$[90_2^0/0_2^0/\pm 45_2^0]_s$

Bending-stretching coupling coefficients (B_{ij}) of all lay-ups vanish, because all six lay-ups, given in Table 1, have symmetric stacking sequence arrangement with respect to mid plane of the shell wall. Extensional stiffness coefficients (A_{ij}) of the six different lay-ups are identical, because extensional stiffness coefficients do not depend on the ply arrangement within the shell wall. Similarly, transverse shear stiffness coefficients of the lay-ups are also identical, because shear moduli of the ply material are same, and the use of 0^o, $\pm 45^o$, and 90^o orientations result in identical transverse shear stiffness coefficients. On the other hand, bending stiffness coefficients (D_{ij}) depend on the ply arrangement through the thickness of the shell wall. For the six different lay-ups, Fig.6 compares the scaled non-dimensional bending stiffness coefficients which are calculated by Eq. 21.

$$\mathrm{Dij} = (D_{ij} / E_1 h^3) * 10^3 \quad (i, j = 1,2,6) \qquad (21)$$

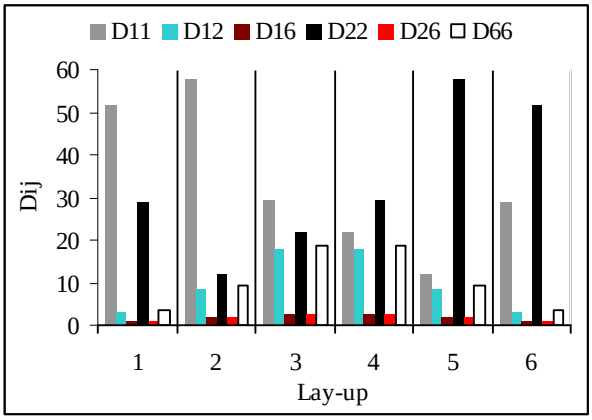

Fig.6. Bending stiffness coefficients (Table 1)

It should be noted that since the extensional and transverse shear stiffness coefficients of the lay-ups are identical, the differences in the natural frequencies will be governed by the differences in the bending stiffness coefficients of these lay-ups. Fig. 7 gives the variation of the scaled, non-dimensional fundamental natural frequencies of the lay-ups listed in Table 1, with respect to circumferential wave number.

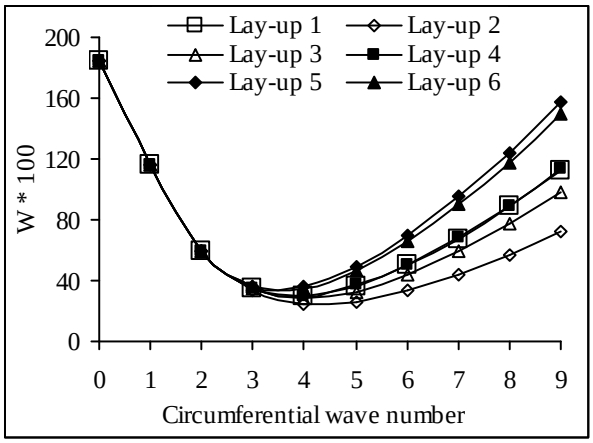

Fig.7. Fundamental natural frequencies of the six different lay-ups given in Table 5

It is noticed that at low circumferential wave numbers, natural frequencies of shells with different lay-ups are almost identical. The differences in the natural frequencies among the lay-ups increase at higher circumferential wave numbers. This

behaviour is again attributed to the fact that, at high circumferential wave numbers, bending strain energy constitutes the major portion of the total strain energy, whereas at low circumferential wave numbers extensional strain energy is more dominant [12]. As a result of this behaviour, the total strain energy shows a somewhat parabolic form. Therefore, variation of natural frequencies of shells of revolution with the circumferential wave number also shows a parabolic form. Since the extensional stiffness coefficients (A_{ij}) of the six lay-ups are identical, at low circumferential wave numbers natural frequencies are very close to each other, such that in Fig. 7 no difference can be observed. However, as the circumferential wave number is increased, the differences in the bending stiffness coefficients start to have effect on the natural frequencies of the shell with different lay-ups. It is seen that bending stiffness coefficient in the circumferential direction (D22) predominantly governs the magnitude of the natural frequency at high circumferential wave numbers. Fig. 6 shows that shell with lay-up 5 has the highest bending stiffness coefficient in the circumferential direction (D22), due to the placement of 90^o and 45^o layers in the outer side of the shell wall. Therefore, at higher circumferential wave numbers, lay-up 5 has the highest natural frequencies. On the other hand, shell with lay-up 2 has the highest bending stiffness along the meridian of the shell (D11), and lowest circumferential bending stiffness (D22), due to the placement of 90^o and 45^o layers inside and 0^o layers outside the shell wall. Therefore, as the circumferential wave number is increased, the largest difference in the natural frequencies occurs between shells with lay-ups 5 and 2. However, it should be expected that at higher axial modes, the difference between the natural frequencies of shells with lay-up 5 and lay-up 2 should gradually diminish. This is because, at higher axial modes, the number of nodal points along the meridian of the shell also increases, and bending stiffness along the shell axis (D11) also starts to play an important role in governing the magnitude of the natural frequency of the shell.

4.3 Effect of Coupling Stiffness Coefficients

The effect of coupling stiffness coefficients on the natural frequencies is studied for a laminated cylindrical shell (radius: 0.21m, length: 1.2 m), which is simply supported at both edges. Table 2 gives the three different stacking sequences, which are used as test cases. Shell wall is assumed to be formed from 0.2 mm thick plies, and ply angles are selected such that the three lay-ups formed symmetric (*Ls*), antisymmetric (*La*), and unsymmetric (*Lu*), shell walls with respect to the middle surface of the shell.

Table 2. List of lay-ups

Lay-up	Stacking sequence
Ls	$[0^o/30^o/90^o/60^o]_{\text{symmetric}}$
La	$[0^o/30^o/90^o/60^o]_{\text{antisymmetric}}$
Lu	$[0^o/30^o/90^o/60^o/0^o/30^o/90^o/60^o]$

For the unsymmetric lay-up case, in order to have all coupling stiffness coefficients non-zero, highly orthotropic Boron/Epoxy is taken as the ply material with E_1 =224GPa, E_2 =12.7GPa, ν_{12} =0.256, $G_{12} = G_{13} = 4.42$ GPa, $G_{23} = 2.48$ GPa ρ =2527 kg m^{-3}.

Figs. 8, 9, 10 and 11 compare the scaled non-dimensional extensional, transverse shear, bending stretching coupling, and bending stiffness coefficients of the three lay-ups listed in Table 2, respectively. Stiffness coefficients are made dimensionless, and scaled according to the following scheme.

$$\text{Aij} = (A_{ij}/(E_1 h))*100 \quad (i, j = 1,2,6) \tag{8}$$

$$\text{Asij} = (As_{ij}/(E_1 h))*100 \quad (i, j = 4,5) \tag{9}$$

$$\text{Bij} = (B_{ij}/(E_1 h^2))*100 \quad (i, j = 1,2,6) \tag{10}$$

$$\text{Dij} = (D_{ij}/(E_1 h^3))*100 \quad (i, j = 1,2,6) \tag{11}$$

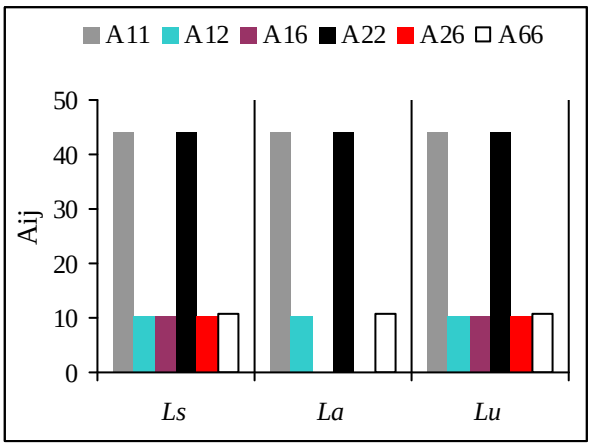

Fig.8. Extensional stiffness coefficients

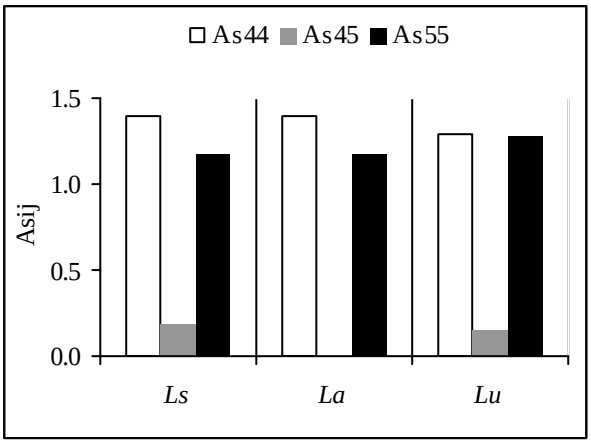

Fig.9. Transverse shear stiffness coefficients

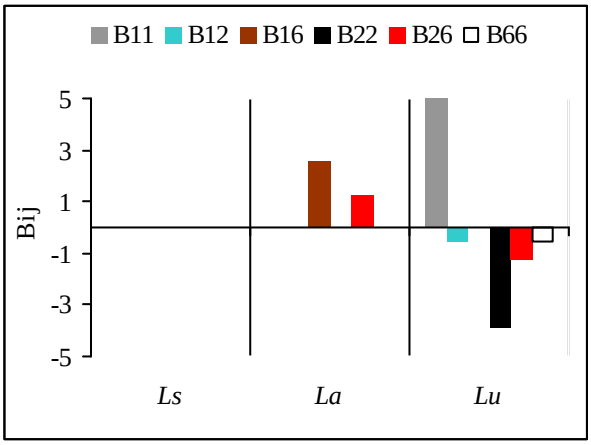

Fig.10. Bending stretching coupling stiffness terms

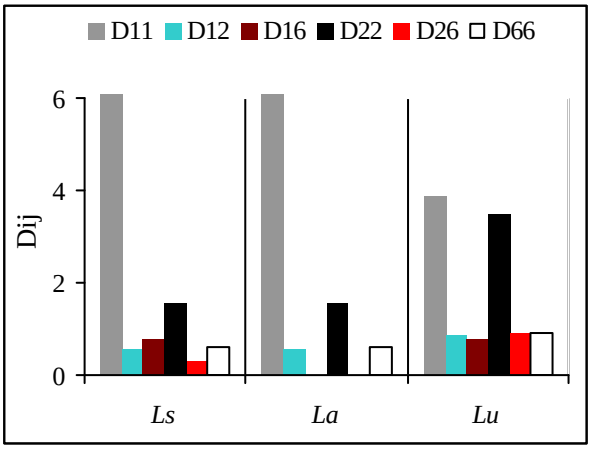

Fig.11. Bending stiffness coefficients

Fig. 12 shows the variation of the natural frequency with respect to circumferential wave number of the shells with symmetric, antisymmetric and unsymmetric lay-ups.

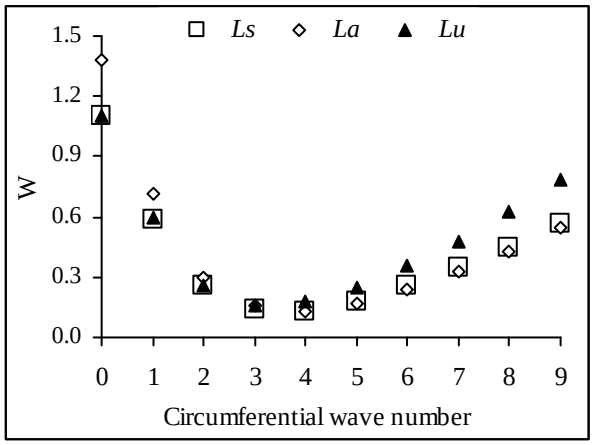

Fig.12. Fundamental frequencies of the cylinders composed of lay-ups given in Table 2

It is noticed that at high circumferential wave numbers, shell with unsymmetric lay-up has higher natural frequencies compared to the shells with symmetric and antisymmetric lay-ups. This difference can be explained when the bending stiffness coefficients of the three lay-ups are compared with each other in Fig. 11. It is seen that the shell with the unsymmetric lay-up has the highest circumferential bending stiffness D22, and therefore due to the dominance of bending strain energy at high circumferential wave numbers, shell with unsymmetric lay-up attained the highest natural frequency. However, this conclusion can not be generalized, because by placing the plies with circumferential fibre orientation on the outer side of the shell wall, circumferential bending stiffness of the symmetric and antisymmetric lay-ups can be made very close to the circumferential bending stiffness of the unsymmetric lay-up. In that case, natural frequencies of the shells with three lay-ups would be very close to each other at high circumferential wave numbers. It should also be noticed that for the unsymmetric lay-up, due to the existence of coupling terms, shell is more flexible. However, it is seen that the bending stiffness coefficient D22 is more effective on the natural frequencies compared to the effect of coupling terms and as a result, natural frequencies increase.

Fig. 12 shows that at the low circumferential wave numbers, shell with antisymmetric lay-up has higher natural frequencies compared to shells with symmetric and unsymmetric lay-ups. Fig. 8 shows that all three lay-ups have the same extensional stiffness coefficients except for the absence of stretching-shearing coupling coefficients in the antisymmetric lay-up. Because of the dominance of extensional strain energy at low circumferential

wave numbers, natural frequencies are mainly governed by the extensional stiffness coefficients. Therefore, at low circumferential wave numbers, the increase in the natural frequencies of the shell with antisymmetric lay-up is attributed to the absence of the stretching-shearing coupling (A16,A26). Coupling terms effectively make the shell more flexible, and they cause decrease in the natural frequencies.

The dominance of extensional strain energy at low circumferential wave numbers can also be verified, when the natural frequencies of shells with symmetric and unsymmetric lay-ups are compared with each other in Fig. 12. Fig. 12 shows that at low circumferential wave numbers, natural frequencies of shells with symmetric and unsymmetric lay-ups are almost equal to each other. On the other hand, Figs. 8, 9, 10 and 11 show that these lay-ups have different bending-stretching coupling coefficients, and bending stiffness coefficients, but they have the same extensional stiffness coefficients. Since the extensional stiffness coefficients predominantly govern the extensional strain energy, frequency calculations also verify the dominance of extensional strain energy at low circumferential wave numbers.

Further study of the effect of coupling stiffness coefficients on the natural frequencies is demonstrated for the cylindrical shell with the unsymmetric lay-up given in Table 2. The natural frequencies of the cylinder with unsymmetric lay-up are compared with the natural frequencies of the cylinder with a hypothetical lay-up, in which all the coupling terms are made null. These coupling terms include all bending-stretching coupling stiffness coefficients Bij, extensional and bending stiffness coefficients with subscripts 16, 26, and transverse shear stiffness coefficient with subscript 45. When the coupling terms are omitted, the resulting shell equations become same as the orthotropic lay-up case, for which simpler solutions can be obtained. Fundamental natural frequencies of the cylinder composed of the unsymmetric lay-up, with and without coupling terms, are compared in Fig. 13 for different circumferential wave numbers. Numerical results are obtained for two cylinders, which are clamped and simply supported at both ends, respectively.

Fig. 13 shows that when the coupling terms are omitted in the analysis, natural frequencies increase as expected. Although the difference between the natural frequencies is not very high, the higher difference encountered in the natural frequencies at low circumferential wave numbers can not be neglected in free vibration and dynamic loading problems.

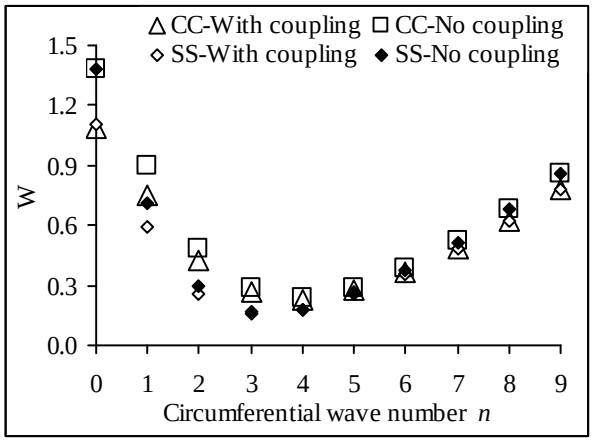

Fig. 13. Effect of coupling terms on the frequencies: CC: Clamped-clamped, SS: Simply supported

It should also be noted that at higher circumferential wave numbers, the effect of boundary conditions diminishes, and the natural frequencies get very close to each other. This behaviour is also expected, because at high circumferential wave numbers, the total number of nodal points around the circumference of the shell is twice the circumferential wave number. Therefore, the shell actually can not feel the difference between the simply supported and clamped edge conditions.

5 Conclusion

The effect of anisotropy on the vibration characteristics of laminated composite shells of revolution is studied by a semi-analytical solution method, which exploits the combination of the numerical integration technique, and a modified frequency trial method. The fundamental system of shell of revolution equations are derived by utilizing the governing equations of anisotropic shells of revolution, including first order transverse shear deformation, and all components of translatory and rotary inertia.

Numerical results are presented on the effect of fibre orientation angle, stacking sequence, and coupling stiffness coefficients on the natural frequencies and modes shapes of anisotropic shells of revolution. Results are obtained for different shell geometries with different boundary conditions to show the generality of the solution method. It has been observed that shell geometry and boundary conditions can have a significant impact on how the fibre orientation angle affects the stiffness of the

shell of revolution, thus the natural frequencies. It is shown that at sufficiently high circumferential wave numbers, shells with layers having circumferential fibre orientation start to have higher natural frequencies irrespective of the boundary conditions imposed.

Based on the results obtained in present study, it can be inferred that at the low circumferential modes, extensional stiffness coefficients govern the magnitude of the fundamental natural frequency, whereas at the higher circumferential wave numbers, bending stiffness coefficients become the dominating factor. This finding actually verifies the dominance of extensional strain energy at low circumferential wave numbers, and the dominance of bending strain energy at high circumferential wave numbers, as indicated by Arnold and Warburton [12]. Thus, for anisotropic shells of revolution with different shell wall lay-ups, it is possible to compare the natural frequencies by of the shells qualitatively, simply by comparing the stiffness coefficients for the particular circumferential wave number. The qualitative comparison can be very reliable at low and high circumferential wave numbers. Such a qualitative comparison may aid alternative lay-up design decisions to be made relatively easily and faster, for composite shells of revolution that are expected to be exposed to different dynamic load environment.

Results of the present study also show that the coupling stiffness coefficients reduce the fundamental natural frequencies. This conclusion is expected because of the higher flexibility of the shell of revolution due to the coupling terms. In addition, it was also observed that the effect of coupling stiffness coefficients of anisotropic shells of revolution on the fundamental natural frequencies decrease at high circumferential wave numbers. Therefore, at high circumferential wave numbers, the use of orthotropic material models, which can be obtained by omitting the coupling stiffness coefficients of the anisotropic shell of revolution, can give very close results for the fundamental natural frequencies of anisotropic shells of revolution. However, at low circumferential wave numbers, coupling terms may have significant effect on the natural frequencies. Therefore, the effect of coupling stiffness coefficients on the fundamental natural frequencies can not be disregarded, for the free vibration and dynamic loading problems involving anisotropic shells of revolution.

References

[1] Noor A.K. and Peters J.M. “Vibration analysis of laminated anisotropic shells of revolutions”. *Computer Methods in Applied Mechanics and Engineering,* Vol. 61, pp 277-301, 1987.

[2] Tımarcı T. and Soldatos K.P. “Vibrations of angle-ply laminated circular cylindrical shells subjected to different sets of edge boundary conditions”. *Journal of Engineering Mathematics,* Vol. 37, pp 211-230, 2000.

[3] Xi Z.C., Yam L.H. and Leung T.P. “Semi-analytical study of free vibration of composite shells of revolution based on the Reissner-Mindlin assumption”. *International Journal of Solids and Structures*, Vol.33, pp 851-863, 1996.

[4] Correia I.F., Barbosa J.I., Soares C.M.M. and Soares C.A.M. “A finite element semi-analytical model for laminated axisymmetric shells: statics, dynamics and buckling”. *Computers and Structures,* Vol. 76, pp 299-317, 2000.

[5] Tan D.Y. “Free vibration analysis of shells of revolution”. *Journal of Sound and Vibration,* Vol. 213, pp 15-33, 1998.

[6] Yavuzbalkan E. “Free Vibration Analysis of Anisotropic Laminated Composite Shells of Revolution”. MSc Thesis, Department of Aerospace Engineering, Middle East Technical University, Ankara, Turkey, 2005.

[7] Reissner E. “A new derivation of the equations for the deformation of elastic shells”. *American Journal of Mathematics,* Vol. 63, pp 177-184, 1941.

[8] Toorani M.H. and Lakis A.A. “General equations of anisotropic plates and shells including transverse shear deformations, rotatory inertia and initial curvature effects”. *Journal of Sound and Vibration,* Vol. 237, pp 561-615, 2000.

[9] Vinson J.R. and Sierakowski R.L. “*The behaviour of structures composed of composite materials*”. 2nd edition, Kluwer Academic Publishers, Dordrecht, The Netherlands, 2002.

[10] Soedel W. “*Vibration of shells and plates*”. Marcel Dekker, New York, 1993.

[11] Kalnins A. “Free vibration of rotationally symmetric shells”. *Journal of the Acoustical Society of America,* Vol. 36, pp 1355-1365, 1964.

[12] Arnold R.N. and Warburton G.B. “Flexural vibrations of the walls of thin cylindrical shells having freely supported ends”. *Proceedings of the Royal Society of London, Series A, Mathematical and Physical Sciences,* Vol. 197, pp 238-256, 1949.